

A DFT Study of Site-Selectivity in Oxidative Addition Reactions with Pd⁰ Complexes: The Effect of an Azine Nitrogen and the Use of Different Types of Halogen Atoms in the Substrate

Wouter A. Herrebout,^[a] Nick Nagels,^[a] Stefan Verbeeck,^[a] Benjamin J. van der Veken,^[a] and Bert U. W. Maes*^[a]

Keywords: Oxidative addition / Palladium / Selectivity / Density functional calculations

The site-selectivity of Pd-catalyzed reactions of 2,3-dihalopyridines [2,3-dichloropyridine (**1**), 2,3-dibromopyridine (**3**) and 2-chloro-3-iodopyridine (**2**)] has been studied by computing the oxidative addition process using DFT calculations. The activating effect of the azine nitrogen atom on C(2) and C(3) has been obtained by comparison with the corresponding dihalobenzene [1,2-dichlorobenzene (**4**), 1,2-dibromobenzene (**5**) and 1-chloro-2-iodobenzene (**6**)]. The performed calculations

involve the use of Pd(PPh₃)₂, Pd(BINAP) and Pd(XANTPHOS) as catalysts. The formation of pre-reactive complexes proved to be a very important factor in the determination of the activation energy values. A comparison with the simplified systems Pd(PPh₃)₂, Pd(H-BINAP) and Pd(H-XANTPHOS) revealed that care has to be taken when simplified catalyst systems are used for the simulation of the oxidative addition process.

Introduction

Pd-catalyzed reactions such as the Suzuki–Miyaura, Migita–Kosugi–Stille, Buchwald–Hartwig and Mizoroki–Heck reaction have caused a revolution in organic chemistry in the last decades.^[1] While these processes have historically been developed on carbocycles the interest in Pd-catalyzed reactions for the decoration and construction of heterocycles is a more recent phenomenon.^[2] This shift is obvious if one takes into account that the majority of drugs and agrochemicals contain a heterocycle as subunit. The usually high functional group compatibility of Pd-mediated reactions make them a suitable tool to couple highly functionalized subunits in the synthesis of complex natural products and to perform efficient lead optimization in medicinal chemistry/agrochemistry programs. This chemistry is certainly not limited to discovery research. In the last years in all major pharmaceutical and agrochemical companies Pd-catalyzed reactions have been executed on kilogram-to-few-hundred kilogram scale in the frame of the development of new drug/agrochemical candidates.^[2a,3] There are not so many known examples of the use of Pd-catalyzed reactions in production processes yet. A striking example of large scale production is the synthesis of the launched fungicide Boscalid [2-chloro-*N*-(4'-chlorobiphenyl-2-yl)nicotinamide] by BASF. The biphenyl unit of Boscalid is currently prepared in Brazil via Suzuki reaction on a huge scale.^[3d]

An important part of the Pd-catalyzed processes mechanistically starts with an oxidative addition reaction in which the Pd⁰ catalyst inserts into the carbon-(pseudo)halogen bond and changes to oxidation state +II. Although many experimental and more recently theoretical studies have focused on the mechanism of oxidative addition of aryl halides to Pd⁰ complexes,^[4] only two theoretical studies on the site-selectivity of the oxidative addition process on polyhalogenated heterocycles have been reported.^[5] A fundamental insight in the factors governing the selectivity is important as, even when the oxidative addition is not rate limiting in the catalytic cycle, it can still determine the site-selectivity of the Pd-catalyzed reaction studied. There is a great interest in site-selective Pd-catalyzed reactions on polyhalogenated substrates as exemplified by two recent reviews describing cross-coupling reactions with organometallic compounds on nitrogen, oxygen and sulfur containing heteroaromatics.^[6] Selectivity can be achieved in two ways. A first approach uses different types of halogen atoms (Cl, Br, I) on the basis of their different C–X bond strengths. Another possibility is the introduction of substituents on and/or heteroatoms in the aromatic ring. They will govern selectivity between two identical halogen atoms on the basis of their activating or deactivating effect.

The work of our laboratory on site-selective Buchwald–Hartwig reactions of 2,3-dihalopyridines with anilines and aza analogues, as well as the frequent presence of the pyridine nucleus in drugs and agrochemicals, prompted us to select these substrates as models for a prediction of the site-selectivity in the oxidative addition via density functional theory (DFT) calculations. Earlier we found that 2,3-dichlo-

[a] Department of Chemistry, University of Antwerp, Groenenborgerlaan 171, 2020 Antwerp, Belgium
Fax: +32-32653233
E-mail: bert.maes@ua.ac.be

Supporting information for this article is available on the WWW under <http://dx.doi.org/10.1002/ejoc.200900808>.

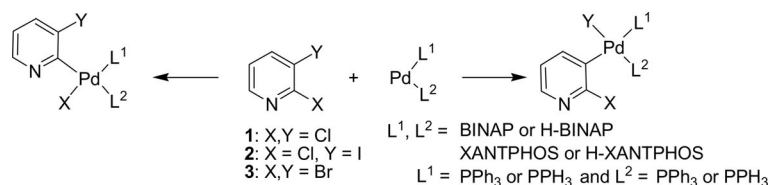


Figure 1. Oxidative addition of 2,3-dihalopyridines **1–3** with Pd(PPh₃)₂, Pd(BINAP) and Pd(XANTPHOS) and Pd(PH₃)₂, Pd(H-BINAP) and Pd(H-XANTPHOS).

ropyridine (**1**) undergoes C-2-selective functionalization while the use of 2-chloro-3-iodopyridine (**2**) allows to synthesize the C-3 regioisomers.^[7,8] 2,3-Dibromopyridine (**3**) gives the same selectivity as **1**.^[9] Besides C–N bond formation also other site-selective Pd-catalyzed reactions have been reported in the literature on **1–3** including Suzuki–Miyaura, Migita–Kosugi–Stille, Negishi, Sonogashira, Mizoroki–Heck and carbonylation reactions.^[10] For all reactions, the same site-selectivity was observed as in our C–N bond forming reactions. The Buchwald–Hartwig reactions on **1–3** performed in our laboratory involved the use of *rac*-BINAP [BINAP: 2,2'-bis(diphenylphosphanyl)-1,1'-binaphthyl] as ligand, for **1** and **2**, and XANTPHOS [XANTPHOS: (9,9-dimethyl-9H-xanthene-4,5-diyl)diphenylphosphane], for **2** and **3**. Initially, we opted to keep the backbones of these bidentate ligands in our DFT calculations and replace the phenyl groups on phosphorus by hydrogen atoms to reduce the computational effort {H-BINAP [H-BINAP: 2,2'-bis(phosphanyl)-1,1'-binaphthyl] and H-XANTPHOS [H-XANTPHOS: (9,9-dimethyl-9H-xanthene-4,5-diyl)diphosphane]}. Such a substitution of phenyl groups by hydrogen atoms, or by methyl groups, in phosphorus based ligands is a common practice in DFT calculations simulating the oxidative addition process.^[4c–4h] The full backbone of a bidentate phosphane ligand in reaction profiling is usually also not kept and simulated by using an alkyl chain or a biphenyl moiety as mimic.^[4h] This most probably is due to the fact that without access to supercomputing facilities even simplified systems with hydrogens or methyl groups on the phosphorus atom in which the actual ligand backbones are kept, are already too large for a full quantum chemical investigation of all the possible reaction pathways at a level of suitable accuracy. In order to check the significance of calculations performed with H-BINAP and H-XANTPHOS test calculations on **1** involving BINAP and XANTPHOS were also performed. Interestingly, these revealed that site-selectivities are still qualitatively correctly predicted but the activation energy values can differ seriously. Based on this finding we decided to perform site-selectivity calculations with simplified H-BINAP and H-XANTPHOS as well as with unaltered BINAP and XANTPHOS (Figure 1).^[11,12] Calculations with PH₃ and PPh₃ were also performed for comparison as PPh₃ is the simplest triarylphosphane ligand which has also been often used in Pd-catalyzed reactions on **1–3** (Figure 1).

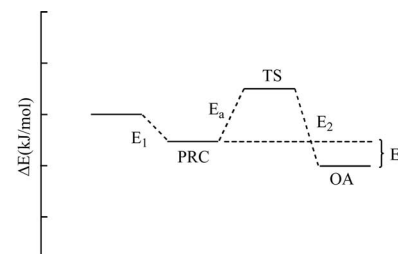
Computational Details

B3LYP density functional calculations were performed by using Gaussian03,^[13] as installed on the CalcUA computing facilities. For C, H, N and O, the 6-31G* basis and for Cl, Br and I the LanL2DZ augmented by one set of six d polarization functions (LANL2DZ*) was used. P and Pd were described using the LanL2DZ basis set. To be able to fully characterize the reaction profiles studied, in the first step of the calculations geometry optimizations were performed for the two interacting monomer units and for the resulting pre-reactive complex. Subsequently, the transition state was obtained by using the QST3 Synchronous Transition Guided Quasi-Newton (STQN) Method.^[14] The geometry optimizations performed for the interacting monomer units allow the correction for Basis Set Superposition Errors and their effect upon the calculated energy barriers, typical errors introduced during the calculations being in the order of 5 to 10 kJ/mol. Such calculations also allowed correcting for the occurrence of pre-reactive complexes. The nature of all transition states was verified using a vibrational frequency calculation. For all structures obtained, a single imaginary frequency was found.

The B3LYP equilibrium geometries for the pre-reactive complexes (PRC), the transition states (TS) and the oxidative addition reaction products (OA) for reaction at C(2) and C(3) of **1–3** with Pd(PPh₃)₂, Pd(BINAP) and Pd(XANTPHOS) as catalysts are shown in Figures S1–S6 in the Supporting Information. The corresponding reaction energy profiles are given in Table 1. For comparison the energy profiles of the analogous reactions involving Pd(PH₃)₂, Pd(H-BINAP) and Pd(H-XANTPHOS) are also incorporated in Table 1.

To obtain information on the applicability of the relatively small basis sets used in the first series of calculations, for a set of complexes, additional geometry optimizations were performed in which the C and H atoms were described using the def2-SVP basis set^[15] and all other atom atoms, including Pd, P and the different halogens, were described using the triple zeta plus polarization def2-TZVP basis set.^[16] In addition, single point calculations were performed in which all atoms are described using the larger basis set. To ensure a more correct description of the dispersion interactions present in the backbone corrections for these interactions were estimated using the empirical method devel-

Table 1. Stabilization energies E_1 (kJ/mol),^[22] activation energies E_a (kJ/mol), energy losses E_2 (kJ/mol) and reaction energies E_r (kJ/mol) for the reaction of **1–6** with Pd(PH₃)₂, Pd(H-BINAP) and Pd(H-XANTPHOS) and Pd(PPh₃)₂, Pd(BINAP) and Pd(XANTPHOS). All values refer to potential energy. PRC: pre-reactive complex, TS: transition state, OA: oxidative addition reaction product.



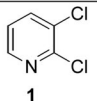
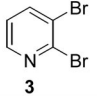
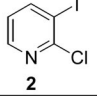
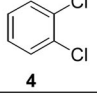
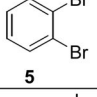
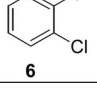
	PPh ₃	PH ₃	BINAP	H-BINAP	XANTPHOS	H-XANTPHOS
1						
E_1	-18.1	-6.8	-28.3	-8.0	-12.3	-6.3
E_a	83.2	65.8	25.8	30.1	51.4	37.2
E_2	-112.0	-105.0	-112.3	-108.2	-113.6	-107.6
E_r	-28.8	-39.2	-86.5	-78.1	-62.2	-70.4
1 C(2)						
E_1	-9.3	-6.2	-40.3	-8.1	-20.6	-7.4
E_a	100.4	79.1	67.4	43.0	72.3	49.9
E_2	-138.9	-131.4	-137.4	-132.7	-120.2	-114.3
E_r	-38.5	-52.3	-70.0	-89.7	-47.9	-64.4
3						
E_1	-17.3	-14.2	-31.5	-13.2	-11.6	-10.7
E_a	61.5	44.4	9.5	18.3	35.3	23.3
E_2	-81.2	-78.4	-93.4	-98.0	-115.9	-125.4
E_r	-19.7	-34.0	-83.9	-79.7	-80.6	-102.1
3 C(2)						
E_1	-8.6	-10.7	-34.4	-13.4	-14.5	-14.9
E_a	77.6	56.5	38.1	29.7	44.1	33.4
E_2	-130.1	-130.1	-136.9	-136.9	-111.0	-111.0
E_r	-52.5	-73.6	-98.8	-107.2	-66.9	-77.6
2						
E_1	-18.0	-6.4	-25.1	-7.2	-5.5	-7.0
E_a	90.4	67.2	27.5	30.7	48.5	38.5
E_2	-83.3	-109.0	-93.1	-114.8	-114.9	-114.5
E_r	7.1	-41.8	-65.6	-84.1	-66.4	-76.0
2 C(2)						
E_1	-15.7	-16.6	-44.8	-30.9	-16.6	-30.4
E_a	66.9	41.0	25.9	22.9	25.2	23.7
E_2	-121.7	-111.4	-124.0	-134.4	-98.9	-120.8
E_r	-54.8	-70.4	-98.1	-111.5	-73.7	-97.1
2 C(3)						
E_1	-9.5	-7.7	-28.3	-13.8	-11.0	-10.5
E_a	129.2	85.6	59.8	51.2	75.0	58.3
E_2	-136.3	-124.6	-135.8	-117.5	-124.6	-121.4
E_r	-7.1	-39.0	-76.0	-66.3	-49.6	-63.1
4						
E_1	-9.2	-12.4	-22.7	-14.3	-10.0	-11.2
E_a	81.4	60.8	34.1	43.6	48.6	45.1
E_2	-121.1	-125.4	-130.4	-122.7	-108.7	-128.9
E_r	-39.7	-64.6	-96.3	-79.1	-60.1	-83.8
5						
E_1	-9.3	-7.3	-26.2	-6.8	-10.2	-9.4
E_a	102.8	91.6	61.7	54.5	77.0	61.3
E_2	-178.5	-135.4	-131.5	-122.6	-126.3	-123.7
E_r	-75.7	-43.8	-69.8	-68.1	-49.3	-62.4
6 C(1)						
E_1	-11.3	-15.2	-47.4	-14.7	-22.9	-17.8
E_a	59.1	36.7	42.8	23.2	40.0	31.0
E_2	-76.8	-83.8	-124.6	-117.7	-98.8	-101.7
E_r	-17.7	-47.2	-81.8	-94.5	-58.8	-70.7
6 C(2)						

oped by Grimme.^[17] To reduce CPU requirements, the larger basis set calculations were performed using Turbomole 6.0.^[18] For all calculations, standard B3LYP functionals were used in combination with the resolution of identity (RI-DFT) approximation.^[19]

Results and Discussion

First we computed the site-selectivity in 2,3-dihalopyridines containing two identical halogen atoms (**1**, **3**). The calculated C(2) and C(3) activation energies (kJ/mol), $E_a[C(2)]$ and $E_a[C(3)]$, involving the different catalysts are summarized in Table 2. Interestingly, the $\Delta E_a[C(3)-C(2)]$ is relatively high (ca. 10–40 kJ/mol) for Pd(PPh₃)₂, Pd(BINAP) and Pd(XANTPHOS) which is in agreement with the site-selectivity observed experimentally in Pd-catalyzed reactions on **1** and **3** using Pd-catalysts based on these ligands.^[7,9,10] There is a significant $\Delta E_a[C(3)-C(2)]$ difference for Pd(BINAP) and Pd(XANTPHOS) for substrate **1** as well as **3**. This difference does not reveal from the calculations involving Pd(H-BINAP) and Pd(H-XANTPHOS). A calculation involving Pd(PPh₃)₂ gave an $\Delta E_a[C(3)-C(2)]$ which is similar as obtained for XANTPHOS as ligand. Interestingly, Pd(PH₃)₂ and Pd(PPh₃)₂ gave small $\Delta E_a[C(3)-C(2)]$ differences. Our calculations on **1** and **3** show that, for these substrates, qualitative site-selectivity predictions can be achieved for the three ligands under study with simple PH₃ as model ligand for the palladium catalyst. For Pd(PPh₃)₂ and Pd(XANTPHOS) as catalysts, Pd(PH₃)₂ interestingly also gives a fairly good quantitative idea (**1**: 13.3 for PH₃ vs. 20.9 kJ/mol for XANTPHOS; **3**: 12.1 for PH₃ vs. 8.8 kJ/mol for XANTPHOS). However, Pd(PH₃)₂ seriously underestimates the site-selectivity for Pd(BINAP) (**1**: 13.3 for PH₃ vs. 41.6 kJ/mol for BINAP; **3**: 12.1 for PH₃ vs. 28.6 kJ/mol for BINAP). As expected, based on published calculated effects of model bidentate ligands on oxidative addition energies, the $E_a[C(2)]$ and $E_a[C(3)]$ values are much higher for Pd(PPh₃)₂ than for Pd(BINAP) and Pd(XANTPHOS) in substrate **1** and **3** supporting a higher reactivity in oxidative addition reactions of the latter two.^[20] This trend can also be seen upon comparison of Pd(PH₃)₂, Pd(H-BINAP) and Pd(H-XANTPHOS). Important to note is that there seems to be no significant $\Delta E_a[C(3)-C(2)]$ difference between a substrate containing two chlorine atoms (**1**) or two bromine atoms (**3**) with Pd(PPh₃)₂ (17.2 vs. 16.1 kJ/mol). With Pd(BINAP) and Pd(XANTPHOS) a significantly larger difference is observed when two chlorine atoms instead of two bromine atoms are present (BINAP: 41.6 vs. 28.6 kJ/mol; XANTPHOS: 20.9 vs. 8.8 kJ/mol). For Pd(H-BINAP) and Pd(H-XANTPHOS) we could not identify a significant $\Delta E_a[C(3)-C(2)]$ difference for the dichloro- and dibromopyridine substrate (H-BINAP: 12.9 vs. 11.4 kJ/mol; H-XANTPHOS: 12.7 vs. 10.1 kJ/mol). The $E_a[C(3)]$ for oxidative addition with a bidentate ligand based catalyst seems to be similar irrespective of the ligand used. This can be observed in substrate **1** as well as **3** upon comparison of the energies computed for Pd(BINAP) and Pd(XANTPHOS). The significant differences in $\Delta E_a[C(3)-C(2)]$ observed for both bidentate ligands are therefore solely determined by $E_a[C(2)]$ in these substrates. For the simplified systems Pd(H-BINAP) and Pd(H-XANTPHOS) only a small difference in $E_a[C(2)]$ value could be observed. In order to determine the effect on the activation energy of the nitrogen

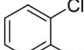
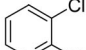
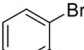
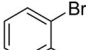
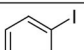
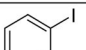
Table 2. Activation energies E_a (kJ/mol) and differences in activation energies ΔE_a (kJ/mol) between C(3) and C(2) for the reactions of **1–6**, with Pd(PPh₃)₂, Pd(BINAP) and Pd(XANTPHOS) and Pd(PH₃)₂, Pd(H-BINAP) and Pd(H-XANTPHOS). All values refer to potential energy.

		PPh ₃	PH ₃	BINAP	H-BINAP	XANTPHOS	H-XANTPHOS
 1	$E_a[\text{C}(3)]$	100.4	79.1	67.4	43.0	72.3	49.9
	$E_a[\text{C}(2)]$	83.2	65.8	25.8	30.1	51.4	37.2
	$\Delta E_a[\text{C}(3) - \text{C}(2)]$	17.2	13.3	41.6	12.9	20.9	12.7
 3	$E_a[\text{C}(3)]$	77.6	56.5	38.1	29.7	44.1	33.4
	$E_a[\text{C}(2)]$	61.5	44.4	9.5	18.3	35.3	23.3
	$\Delta E_a[\text{C}(3) - \text{C}(2)]$	16.1	12.1	28.6	11.4	8.8	10.1
 2	$E_a[\text{C}(3)]$	66.7	41.0	25.9	22.9	25.2	23.7
	$E_a[\text{C}(2)]$	90.4	67.2	27.5	30.7	48.5	38.5
	$\Delta E_a[\text{C}(3) - \text{C}(2)]$	–23.7	–26.2	–1.6	–7.8	–23.3	–14.8
 4	$E_a[\text{C}(1), \text{C}(2)]$	129.2	85.6	59.8	51.2	75.0	58.3
 5	$E_a[\text{C}(1), \text{C}(2)]$	81.4	60.8	34.1	43.6	48.6	45.1
 6	$E_a[\text{C}(2)]$	59.1	36.7	42.8	23.2	39.9	31.0
	$E_a[\text{C}(1)]$	102.8	91.6	61.7	54.5	77.0	61.3

atom on C(3) vs. C(2) of the 2,3-dihalopyridine, we calculated the activation energy required for oxidative addition of one of the carbon–halogen bonds of 2,3-dichlorobenzene (**4**) and 2,3-dibromobenzene (**5**) to the same bidentate ligand based catalysts (Table 2). When one subtracts from the $E_a[\text{C}(X)]$ values obtained for reaction at C(X) in **4** and **5** the $E_a[\text{C}(X)]$ values for reaction at C(2) and C(3) in the corresponding 2,3-dihalopyridines, the activation effect of nitrogen can be quantified (Table 3). This revealed that for **1** the activating effect of the nitrogen atom is larger at C(2) than at C(3) irrespective of the bidentate ligand (BINAP, XANTPHOS) used. For **3** the same observation was made, but the activating effect at C(2) seems to be smaller for this substrate (BINAP: 24.6 kJ/mol for **3** vs. 34.0 kJ/mol for **1**; XANTPHOS: 13.3 kJ/mol for **3** vs. 23.6 kJ/mol for **1**). Calculations performed with Pd(PPh₃)₂ showed also in this case that the activating effect of nitrogen is larger at C(2) than at C(3). Again, the activating effect in the chlorinated substrate (46 kJ/mol) seems to be larger than in the brominated (19.9 kJ/mol) substrate for C(2). Both for substrate **1** and **3** there is no significant activating effect of the nitrogen atom at C(3) for all ligands except in one case: substrate **1** with Pd(PPh₃)₂ catalyst (28.8 kJ/mol). The reason for the presence of this effect in substrate **1** and its absence in substrate **3** remains unclear.

Secondly, we computed the site-selectivity in 2-chloro-3-iodopyridine (**2**). The calculated $E_a[\text{C}(2)]$ and $E_a[\text{C}(3)]$ values (kJ/mol) involving the different catalysts are summarized in Table 2. The activation energies, for Pd(PPh₃)₂, Pd(BINAP) and Pd(XANTPHOS), are in favor of reaction at C(3) which is in agreement with the experimentally observed site-selectivity on **2**.^[8,10] Interestingly, the $\Delta E_a[\text{C}(3) -$

Table 3. Differences in the activation energy ΔE_a (kJ/mol) for the reactions of dihalopyridines (**1**, **3**, **2**) and the corresponding dihalobenzenes (**4**, **5**, **6**) with Pd(PPh₃)₂, Pd(BINAP) and Pd(XANTPHOS). All values refer to potential energy.

		PPh ₃ BINAP XANTPHOS			
		$\Delta E_a[\text{C}(1') - \text{C}(3)]$	28.8	−7.6	2.7
		$\Delta E_a[\text{C}(1') - \text{C}(2)]$	46.0	34.0	23.6
4	1				
<hr/>					
		$\Delta E_a[\text{C}(1') - \text{C}(3)]$	3.8	−4.0	4.5
		$\Delta E_a[\text{C}(1') - \text{C}(2)]$	19.9	24.6	13.3
5	3				
<hr/>					
		$\Delta E_a[\text{C}(2') - \text{C}(3)]$	−7.6	16.9	14.7
		$\Delta E_a[\text{C}(1') - \text{C}(2)]$	12.4	34.2	28.5
6	2				

C(2)] difference for Pd(BINAP) (–1.6 kJ/mol) is much smaller than the value obtained for Pd(XANTPHOS) (–23.3 kJ/mol), which is the opposite of what was observed for substrates containing two identical halogen atoms (**1**, **3**). This also reveals from the calculations involving Pd(H-BINAP) and Pd(H-XANTPHOS). Calculation of the $E_a[\text{C}(2)]$ and $E_a[\text{C}(3)]$ values for oxidative addition of **2** to Pd(PPh₃)₂ as catalyst showed that, as observed for **1** and **3**, the $\Delta E_a[\text{C}(3) - \text{C}(2)]$ is similar as computed for Pd(XANTPHOS) but now quantitatively overestimates the site-selectivity induced by Pd(BINAP) (–23.7 for PPh₃ vs. –23.3 XANTPHOS and –1.6 kJ/mol for BINAP). PH₃ and PPh₃ gave similar $\Delta E_a[\text{C}(3) - \text{C}(2)]$ values on **2**. Therefore for the three unsimplified ligands a qualitatively, and for XANTPHOS and PPh₃ a quantitatively, correct result can

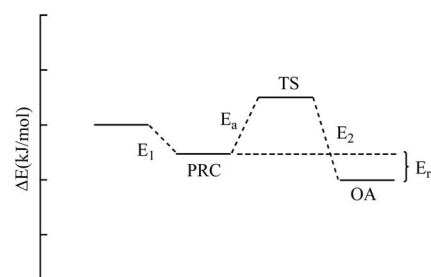
be achieved using PH_3 as model phosphane. In line with the observation on 2,3-dihalopyridines with two identical halogen atoms (**1**, **3**) the $E_{\text{a}}[\text{C}(2)]$ and $E_{\text{a}}[\text{C}(3)]$ values are much higher for $\text{Pd}(\text{PPh}_3)_2$ than for $\text{Pd}(\text{BINAP})$ and $\text{Pd}(\text{XANTPHOS})$ in substrate **2** pointing again to the activating effect of bidentate ligands on the oxidative addition process.^[20] This trend can also be seen upon comparison of $\text{Pd}(\text{PH}_3)_2$, $\text{Pd}(\text{H-BINAP})$ and $\text{Pd}(\text{H-XANTPHOS})$. Comparison of the oxidative addition energies computed for $\text{Pd}(\text{BINAP})$ and $\text{Pd}(\text{XANTPHOS})$ in $\text{C}(3)$ $\{E_{\text{a}}[\text{C}(3)]\}$ as well as $\text{C}(2)$ $\{E_{\text{a}}[\text{C}(2)]\}$ of **2** indicated that the $\Delta E_{\text{a}}[\text{C}(3)-\text{C}(2)]$ observed for the bidentate ligands can solely be ascribed due to a difference in the computed $E_{\text{a}}[\text{C}(2)]$ value, as was also observed for substrates **1** and **3**. For the simplified systems $\text{Pd}(\text{H-BINAP})$ and $\text{Pd}(\text{H-XANTPHOS})$ only a small difference could be observed for the $E_{\text{a}}[\text{C}(2)]$ value. In order to get a quantitative idea of the activating effect of the nitrogen atom on $\text{C}(3)$ vs. $\text{C}(2)$ in **2**, we subtracted the $E_{\text{a}}[\text{C}(X)]$ values for reaction at $\text{C}(2)$ and $\text{C}(3)$ in **2** respectively from the $E_{\text{a}}[\text{C}(X)]$ values obtained for reaction at $\text{C}(1)$ and $\text{C}(2)$ in **6** (Table 3). This revealed that the activating effect of the nitrogen atom is larger for $\text{C}(2)$ than for $\text{C}(3)$ for the three catalyst systems. There is also a significant activating effect of the nitrogen atom on $\text{C}(3)$ for $\text{Pd}(\text{BINAP})$ and $\text{Pd}(\text{XANTPHOS})$ but for $\text{Pd}(\text{PPh}_3)_2$ no significant activating effect was observed for $\text{C}(3)$. This is the reverse of what was observed for **1**. Interestingly, the $E_{\text{a}}[\text{C}(2)]$ of **2** seems not to be influenced by the other *ortho* positioned halogen atom present on the nucleus since the $E_{\text{a}}[\text{C}(2)]$ in **1** and **2** gave only small difference for all three ligands, although in substrate **1** a more electronegative chlorine is present in $\text{C}(3)$ (Table 2). This trend could also be seen with the simplified ligands.

Interestingly, for all substrates pre-reactive complexes (PRC) revealed from the calculations. Their potential occurrence preceding oxidative addition is well documented in the literature.^[4a–4d,4f–4h] For H-BINAP and H-XANTPHOS pre-reactive complexes involving a palladium–iodine bond were observed with substrate **2**. These bidentate model ligands contrast with PH_3 for which no pre-reactive complexes could be identified. Surprisingly, for none of the substrates **1–3** an η^2 arene complex is observed with the simplified ligands PH_3 , H-BINAP , H-XANTPHOS . These results strongly contrast with the data for PPh_3 , BINAP and XANTPHOS for which pre-complexation always occurred. Three types of PRC were observed: pre-reactive complexes involving a palladium–halogen bond, π complexation (η^2 arene) and “hydrogen bonding” via an anagostic interaction of the metal center with the hydrogen of a C–H bond.^[21] In contrast to π complexation, neutral pre-reactive complexes involving palladium–halogen bonding and “hydrogen bonding” have hitherto not been reported to play a significant role. In anionic Pd^0 complexes, however, palladium–iodine as well as anagostic interactions have been predicted earlier.^[4f] Inspection of the equilibrium geometries shown in Figures S1–6 suggest that the exact nature of the pre-reactive complexes is determined by the specific substrate–ligand combination as no general

trends could be deduced. The binding energies of the pre-reactive complexes vary between -5.6 and -48.0 kJ/mol for the palladium–halogen bonding, between -9.5 and -40.0 kJ/mol for the η^2 arene complexes and between -9.3 and -18.1 kJ/mol for the anagostic interactions (Table 1). The latter are only found with PPh_3 as ligand. The anagostic interaction, M–H distance and M–H–C angle, in the pre-reactive complexes in the reaction in $\text{C}(2)$ of **1**, **2**, **3** and in $\text{C}(3)$ of **1** with $\text{Pd}(\text{PPh}_3)_2$ are, respectively, 2.908 Å and 162.4° , 2.806 Å and 162.3° , 2.841 Å and 161.7° , and 3.156 Å and 147.7° . Important to note is that the energies associated with pre complexation are often a significant % of the activation energies required for the actual oxidative addition process. The oxidative addition reaction in $\text{C}(2)$ of **3** with $\text{Pd}(\text{BINAP})$ for example is an extreme case since the stabilization energy (E_1) is more than three times larger than the required activation energy (E_{a}). It should also be stressed that although there are two reaction sites in our 2,3-dihalopyridine substrates each transition state is preceded by its own different pre-reactive complex. If the $\Delta E_{\text{a}}[\text{C}(3)-\text{C}(2)]$ for oxidative addition of the dihalopyridine substrate to a catalyst is very small, the regioselectivity can be governed by the pre complexation process. The reaction of **2** with $\text{Pd}(\text{BINAP})$ might be such a case since the $\Delta E_{\text{a}}[\text{C}(3)-\text{C}(2)]$ is only -1.6 kJ/mol, which simply cannot explain the regioselectivity experimentally observed, while the stabilization energy E_1 is -44.8 kJ/mol for reaction in $\text{C}(3)$ as opposed to a value of -25.1 kJ/mol for reaction in $\text{C}(2)$. This small value for $\Delta E_{\text{a}}[\text{C}(3)-\text{C}(2)]$ might also be the result of the limited basis set used. Therefore we replaced the LANL2DZ(*) basis sets by def2-SVP and def2-TZVP basis sets and repeated geometry optimizations and single point calculations for substrates **1–3** with $\text{Pd}(\text{BINAP})$. The data for the single point calculations in which all atoms are described by using def2-TZVP are summarized in Tables 4 and 5. For substrate **1** the $\Delta E_{\text{a}}[\text{C}(3)-\text{C}(2)]$ values were essentially identical. However, for substrates **2** and **3** substantial differences revealed. Replacing the LANL2DZ(*) basis sets for substrate **2** changed the $\Delta E_{\text{a}}[\text{C}(3)-\text{C}(2)]$ from -1.6 to -13.6 kJ/mol which fits better with the experimental regioselectivity observed for this substrate. The good agreement between calculations involving substrate **1** and the large differences for substrates **2** and **3**, suggest that larger basis sets are able to better describe molecules containing more polarizable atoms such as bromine and iodine.

To further rationalize the different trends reported above, we performed additional calculations in which the relative position of the different frontier orbitals were analyzed, using a similar method as described earlier by Ziegler.^[4h] The results obtained for the 2,3-dihalosubstituted pyridines show that for both the dichloro- (**1**) and the dibromo-substituted species (**3**), the carbon–halogen antibonding molecular orbital is the LUMO+2, while the corresponding carbon–iodine molecular orbital in 2-chloro-3-iodopyridine (**2**) is strongly stabilized and becomes the LUMO. These results fit with the data on chloro-, bromo- and iodobenzene reported by Ziegler.^[4h] The differences and trends observed while comparing the data for $\text{Pd}(\text{PH}_3)_2$, $\text{Pd}(\text{H-BINAP})$ and

Table 4. A comparison of the stabilization energies E_1 (kJ/mol),^[22] activation energies E_a (kJ/mol), energy losses E_2 (kJ/mol) and reaction energies E_r (kJ/mol) for the reaction of **1**, **2** and **3** with Pd(BINAP) calculated with Gaussian and Turbomole. All values refer to potential energy. PRC: pre-reactive complex, TS: transition state, OA: oxidative addition reaction product.



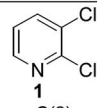
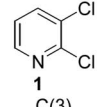
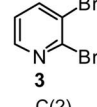
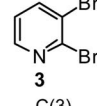
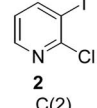
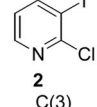
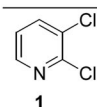
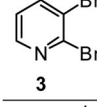
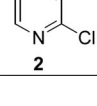
		BINAP Gaussian	BINAP Turbomole
 1 C(2)	E_1	-28.3	-39.6
	E_a	25.8	25.1
	E_2	-112.3	-117.0
	E_r	-86.5	-91.9
 1 C(3)	E_1	-40.3	-49.5
	E_a	67.4	66.8
	E_2	-137.4	-144.3
	E_r	-70.0	-77.5
 3 C(2)	E_1	-31.5	-44.3
	E_a	9.5	6.6
	E_2	-93.4	-93.3
	E_r	-83.9	-86.7
 3 C(3)	E_1	-34.4	-51.9
	E_a	38.1	48.1
	E_2	-136.9	-149.3
	E_r	-98.8	-101.2
 2 C(2)	E_1	-25.1	-65.1
	E_a	27.5	51.4
	E_2	-93.1	-91.5
	E_r	-65.6	-40.1
 2 C(3)	E_1	-44.8	-65.1
	E_a	25.9	37.8
	E_2	-124.0	-129.4
	E_r	-98.1	-91.6

Table 5. A comparison of the activation energies E_a (kJ/mol) and differences in activation energies ΔE_a (kJ/mol) between C(3) and C(2) for the reactions of **1**, **2** and **3** with Pd(BINAP) calculated with Gaussian and Turbomole. All values refer to potential energy.

		BINAP Gaussian	BINAP Turbomole
 1	E_a [C(3)]	67.4	66.8
	E_a [C(2)]	25.8	25.1
	ΔE_a [C(3) - C(2)]	41.6	41.7
 3	E_a [C(3)]	38.1	48.1
	E_a [C(2)]	9.5	6.6
	ΔE_a [C(3) - C(2)]	28.6	41.5
 2	E_a [C(3)]	25.9	37.8
	E_a [C(2)]	27.5	51.4
	ΔE_a [C(3) - C(2)]	-1.6	-13.6

Pd(H-XANTPHOS) as well as Pd(PPh₃)₂, Pd(BINAP) and Pd(XANTPHOS), however, could not be rationalized by comparing the properties of the HOMO molecular orbital and the molecular orbitals located just underneath.

Conclusions

For 2,3-dihalopyridines **1–3** site-selectivities are qualitatively correctly predicted both with Pd catalysts containing the simplified (PH₃, H-BINAP, H-XANTPHOS) and unsimplified (PPh₃, BINAP, XANTPHOS) ligands. The simplest catalyst system Pd(PH₃)₂ can therefore easily be used for this purpose saving significantly CPU usage. Interestingly, quantitatively Pd(PH₃)₂ gives a fairly good ΔE_a [C(3)–C(2)] prediction of the reactions involving oxidative addition of **1–3** to Pd(PPh₃)₂ and Pd(XANTPHOS) but not for Pd(BINAP). This might have a steric origin. The E_a [C(2)] and E_a [C(3)] figures for all dihalopyridine substrates are smaller for bidentate ligands (BINAP, XANTPHOS) than for PPh₃. The same trend can be seen in the three simplified ligands. Comparison of the oxidative addition energies computed for Pd(BINAP) and Pd(XANTPHOS) in C(3) { E_a [C(3)]} as well as C(2) { E_a [C(2)]} of **1–3** indicated that the differences in activation energy { ΔE_a [C(3)–C(2)]} can solely be ascribed due to a difference in the computed E_a [C(2)] value. No such clear difference revealed when comparing with the data obtained for the simplified systems Pd(H-BINAP) and Pd(H-XANTPHOS). To correctly predict oxidative addition energies pre-reactive complexes have to be taken into account [palladium–halogen bonding, π complexation (η^2 arene), “hydrogen bonding” via an agostic interaction]. The energy associated with the pre-reactive complex formation is significant when compared with the activation energies required for the actual oxidative addition process. Our work clearly shows that the use of simplified ligands (replacement of the phenyl groups by hydrogen atoms) can strongly influence the energies and geometries of the prereactive complexes, the transition states and the oxidative addition reaction products. Reliable quantitative data on oxidative addition activation energies can consequently only be obtained by using catalysts which contain the full ligands for the calculations.

Supporting Information (see also the footnote on the first page of this article): Equilibrium geometries for the pre-reactive complexes (PRC), the transition states (TS) and the oxidative addition reaction products (OA) for the reactions computed (Figures S1–S6).

Acknowledgments

We would like to thank the University of Antwerp (NOI BOF UA 2005), the Flemish Government (supercomputing facilities) (Impulsfinanciering van de Vlaamse Overheid voor Strategisch Basisonderzoek PFEU 2003) and the FWO Flanders for financial support and Dr. Caroline Meyers for assistance during the preparation of the manuscript.

[1] *Palladium in Organic Synthesis* (Ed.: J. Tsuji), vol. 14, Springer, Dordrecht, 2005.

- [2] For recent books dealing with the synthesis and construction of heterocycles via Pd-catalysis see: a) *Palladium in Heterocyclic Chemistry* (Eds.: J. J. Li, G. W. Gribble), vol. 26 Pergamon, Amsterdam, **2006**; b) A. Kotschy, G. Timári, *Heterocycles from Transition Metal Catalysis* (Eds.: B. James, P. W. N. M. van Leeuwen), vol. 28, Springer, Dordrecht, **2005**.
- [3] a) S. L. Buchwald, C. Mauger, G. Mignani, U. Scholz, *Adv. Synth. Catal.* **2006**, 348, 23–31; b) J. P. Corbet, G. Mignani, *Chem. Rev.* **2006**, 106, 2651–2710; c) H.-U. Blaser, A. Indolese, F. Naud, U. Nettekoven, A. Schnyder, *Adv. Synth. Catal.* **2004**, 346, 1583–1598; d) A. M. Rouhi, *Chem. Eng. News* **2004**, 82, 49–58; e) C. Torborg, M. Beller, *Adv. Synth. Catal.* **2009**, 351, 3027–3043.
- [4] For recent theoretical studies of the oxidative addition process of aryl halides to mono- and diligated Pd⁰ see: a) R. Fazaeli, A. Ariaifard, S. Jamshidi, E. S. Tabatabaie, K. A. Pishro, *J. Organomet. Chem.* **2007**, 692, 3984–3993; b) K. C. Lam, T. D. Marder, Z. Lin, *Organometallics* **2007**, 26, 758–760; c) M. Ahlquist, P.-O. Norrby, *Organometallics* **2007**, 26, 550–553; d) M. Ahlquist, P. Frstrup, D. Tanner, P.-O. Norrby, *Organometallics* **2006**, 25, 2066–2073; e) A. Ariaifard, Z. Lin, *Organometallics* **2006**, 25, 4030–4033; f) L. J. Goossen, D. Koley, H. Hermann, W. Thiel, *Organometallics* **2005**, 24, 2398–2410; g) L. J. Goossen, D. Koley, H. Hermann, W. Thiel, *Chem. Commun.* **2004**, 2141–2143; h) H. M. Senn, T. Ziegler, *Organometallics* **2004**, 23, 2980–2988.
- [5] a) I. J. S. Fairlamb, C. T. O'Brien, Z. Lin, K. C. Lamb, *Org. Biomol. Chem.* **2006**, 4, 1213–1216; b) C. Y. Legault, Y. Garcia, C. A. Merlic, *J. Am. Chem. Soc.* **2007**, 129, 12664–12665.
- [6] a) I. J. S. Fairlamb, *Chem. Soc. Rev.* **2007**, 36, 1036–1045; b) S. Schroter, C. Stock, T. Bach, *Tetrahedron* **2005**, 61, 2245–2267.
- [7] 2,3-Dichloropyridine: T. H. M. Jonckers, B. U. W. Maes, G. L. F. Lemi re, R. Dommissie, *Tetrahedron* **2001**, 57, 7027–7034.
- [8] 2-Chloro-3-iodopyridine: a) B. U. W. Maes, K. T. J. Loones, T. H. M. Jonckers, G. L. F. Lemi re, R. A. Dommissie, A. Haemers, *Synlett* **2002**, 1995–1998; b) C. Meyers, B. U. W. Maes, K. T. J. Loones, G. Bal, G. L. F. Lemi re, R. A. Dommissie, *J. Org. Chem.* **2004**, 69, 6010–6017; c) K. T. J. Loones, B. U. W. Maes, R. A. Dommissie, G. L. F. Lemi re, *Chem. Commun.* **2004**, 2466–2467; d) G. Rombouts, B. U. W. Maes, T. H. M. Jonckers, K. T. J. Loones, *Org. Synth.* **2007**, 84, 215–221.
- [9] 2,3-Dibromopyridine: K. T. J. Loones, B. U. W. Maes, C. Meyers, J. Deruyter, *J. Org. Chem.* **2006**, 71, 260–264.
- [10] For 2,3-Dichloropyridine see for example: a) D. Najiba, J.-F. Carpentier, Y. Castanet, C. Biot, J. Brocard, A. Mortreux, *Tetrahedron Lett.* **1999**, 40, 3719–3722; b) D. R. Gauthier, R. H. Szumigala, P. G. Dormer, J. D. Armstrong, R. P. Volante, P. J. Reider, *Org. Lett.* **2002**, 4, 375–378; c) N. M. Simkovsky, M. Ermann, S. M. Roberts, D. M. Parry, A. D. Baxter, *J. Chem. Soc. Perkin Trans. 1* **2002**, 1847–1849; d) C. S. Burgey, K. A. Robinson, T. A. Lyle, P. E. J. Sanderson, S. D. Lewis, B. J. Lucas, J. A. Kreuger, R. Singh, C. Miller-Stein, R. B. White, B. Wong, E. A. Lyle, P. D. Williams, C. A. Coburn, B. D. Dorsey, J. C. Barrow, M. T. Stranieri, M. A. Holahan, G. R. Sitko, J. J. Cook, D. R. McMasters, C. M. McDonough, W. M. Sanders, A. A. Wallace, F. C. Clayton, D. Bohn, Y. M. Leonard, T. J. Detwiler, J. J. Lynch, Y. Yan, Z. Chen, L. Kuo, S. J. Gardell, J. A. Shafer, J. P. Vacca, *J. Med. Chem.* **2003**, 46, 461–473; e) E. Maerten, F. Hassouna, S. Couve-Bonnaire, A. Mortreux, J.-F. Carpentier, Y. Castanet, *Synlett* **2003**, 1874–1876; f) J. Albaneze-Walker, C. Bazaral, T. Leavey, P. G. Dormer, J. A. Murry, *Org. Lett.* **2004**, 6, 2097–2100; g) E. Maerten, M. Sauthier, A. Mortreux, Y. Castanet, *Tetrahedron* **2007**, 63, 682–689; h) B. H. Lipshutz, A. R. Abela, *Org. Lett.* **2008**, 10, 5329–5332. For 2-chloro-3-iodopyridine see for example: i) F. Cottet, M. Schlosser, *Eur. J. Org. Chem.* **2002**, 327–330; j) I. Dix, C. Doll, H. Hopf, P. G. Jones, *Eur. J. Org. Chem.* **2002**, 2547–2556; k) A. Bouillon, A. S. Voisin, A. Robic, J.-C. Lancelot, V. Colot, S. Rault, *J. Org. Chem.* **2003**, 68, 10178–10180; l) J. Liu, A. E. Fitzgerald, N. S. Mani, *J. Org. Chem.* **2008**, 73, 2951–2954. For 2,3-dibromopyridine see for example: m) M. Carril, R. SanMartin, E. Dom nguez, I. Tellitu, *Tetrahedron* **2007**, 63, 690–702; n) S. T. Handy, T. Wilson, A. Muth, *J. Org. Chem.* **2007**, 72, 8496–8500.
- [11] For a recent example of all atom DFT calculations involving transition metal complexes consisting of BINAP and XANTPHOS, respectively, see: a) T. Leyssens, D. Peeters, J. N. Harvey, *Organometallics* **2008**, 27, 1514–1523; b) J. D. Hicks, A. M. Hyde, A. M. Cuezva, S. L. Buchwald, *J. Am. Chem. Soc.* **2009**, 131, 16720–16734.
- [12] For an example in which the crucial role of the selection of a phosphane model for rhodium catalysts in hydroformylation reactions has been shown see: M. Torrent, M. Sola, G. Frenking, *Chem. Rev.* **2000**, 100, 439–493.
- [13] M. J. Frisch, G. W. Trucks, H. B. Schlegel, G. E. Scuseria, M. A. Robb, J. R. Cheeseman, J. A. Montgomery Jr., T. Vreven, K. N. Kudin, J. C. Burant, J. M. Millam, S. S. Iyengar, J. Tomasi, V. Barone, B. Mennucci, M. Cossi, G. Scalmani, N. Rega, G. A. Petersson, H. Nakatsuji, M. Hada, M. Ehara, K. Toyota, R. Fukuda, J. Hasegawa, M. Ishida, T. Nakajima, Y. Honda, O. Kitao, H. Nakai, M. Klene, X. Li, J. E. Knox, H. P. Hratchian, J. B. Cross, V. Bakken, C. Adamo, J. Jaramillo, R. Gomperts, R. E. Stratmann, O. Yazyev, A. J. Austin, R. Cammi, C. Pomelli, J. W. Ochterski, P. Y. Ayala, K. Morokuma, G. A. Voth, P. Salvador, J. J. Dannenberg, V. G. Zakrzewski, S. Dapprich, A. D. Daniels, M. C. Strain, O. Farkas, D. K. Malick, A. D. Rabuck, K. Raghavachari, J. B. Foresman, J. V. Ortiz, Q. Cui, A. G. Baboul, S. Clifford, J. Cioslowski, B. B. Stefanov, G. Liu, A. Liashenko, P. Piskorz, I. Komaromi, R. L. Martin, D. J. Fox, T. Keith, M. A. Al-Laham, C. Y. Peng, A. Nanayakkara, M. Challacombe, P. M. W. Gill, B. Johnson, W. Chen, M. W. Wong, C. Gonzalez, J. A. Pople, *Gaussian 03*, Revision C.02, Gaussian, Inc., Wallingford CT, **2004**.
- [14] a) C. Peng, H. B. Schlegel, *Isr. J. Chem.* **1993**, 33, 449–454; b) C. Peng, P. Y. Ayala, H. B. Schlegel, M. J. Frisch, *J. Comput. Chem.* **1996**, 17, 49–56.
- [15] A. Sch fer, H. Horn, R. Ahlrichs, *J. Chem. Phys.* **1992**, 97, 2571–2577.
- [16] a) A. Sch fer, C. Huber, R. Ahlrichs, *J. Chem. Phys.* **1994**, 100, 5829–5835; b) F. Weigend, R. Ahlrichs, *Phys. Chem. Chem. Phys.* **2005**, 7, 3297–3305.
- [17] S. Grimme, *J. Comput. Chem.* **2006**, 27, 1787–1799.
- [18] a) R. Ahlrichs, M. Baer, M. Haeser, H. Horn, C. Koelmel, *Chem. Phys. Lett.* **1989**, 162, 165–169; b) M. Arnim, R. Ahlrichs, *J. Comput. Chem.* **1998**, 19, 1746–1757.
- [19] M. Sierka, A. Hoge Kamp, R. Ahlrichs, *J. Chem. Phys.* **2003**, 118, 9136–9148.
- [20] S. Kozuch, C. Amatore, A. Jutand, S. Shaik, *Organometallics* **2005**, 24, 2319–2330.
- [21] M. Brookhart, M. L. H. Green, G. Parkin, *Proc. Natl. Acad. Sci. USA* **2007**, 104, 6908–6914.
- [22] Pre-reactive complexes: the pre-reactive complexes for substrates 1–3 are shown in Figures S1–6. For dichlorobenzene (**4**) η^2 arene complexation was found for PPh₃, BINAP and XANTPHOS. For dibromobenzene (**5**) a weak anagostic interaction (3.587 Å, 116.9°) was found for PPh₃, while a palladium–bromine bond was observed for the bidentate ligands BINAP and XANTPHOS. For 1-chloro-2-iodobenzene (**6**) for reaction at C(1) an η^2 arene complexation was found for all ligands, while the reactions at C(2) gave an anagostic interaction (3.058 Å, 159.7°) for PPh₃ and palladium–iodine bonding for the bidentate ligands.

Received: July 18, 2009

Revision Received: January 31, 2010

Published Online: April 26, 2010